Theoretical Characterization of the $(H_2O)_{21}$ Cluster: Application of an *n*-body Decomposition Procedure†

Jun Cui, Hanbin Liu, and Kenneth D. Jordan*

Department of Chemistry and Center for Molecular and Materials Simulations, University of Pittsburgh, Pittsburgh, Pennsylvania 15260

Received: November 7, 2005; In Final Form: January 30, 2006

Two low-energy minima of $(H_2O)_{21}$ with very different H-bonding arrangements have been investigated with the B3LYP density functional and RIMP2 methods, as well as with the TIP4P, Dang−Chang, AMOEBA, and TTM2-F force fields. The AMOEBA and TTM2-F model potentials give an energy ordering that agrees with the results of the electronic structure calculations, while the TIP4P and Dang−Chang models give the opposite ordering. Insight into the role of many-body polarization for establishing the relative stability of the two isomers is provided by an *n*-body decomposition of the energies calculated using the various theoretical methods.

1. Introduction

Over the past few years, major strides have been made in understanding the structure and dynamics of water clusters. Recently, there has been renewed interest in the $H^+(H_2O)_{21}$ cluster,[1−5] which appears as a magic number in the mass spectra of $H^+(H_2O)_n$ clusters.[6−9] Over three decades ago, Searcy and Fenn proposed that the $n = 21$ protonated cluster has a structure corresponding to a water dodecahedron with an enclosed water monomer and the excess proton on the surface.[6] Wei and Castleman, on the basis of a titration experiment, offered an alternative interpretation, namely, that the $H^+(H_2O)_{21}$ cluster is comprised of a water dodecahedron with an interior H_3O^+ ion.[7] Comparison of the measured vibrational predissociation spectrum[1,2] with the calculated harmonic vibrational spectra of various isomers leads to the conclusion that the experimentally observed isomer is that originally proposed by Searcy and Fenn with the excess proton on the surface of the cluster.[1−3] Moreover, the calculations indicate that the Searcy−Fenn isomer is the global minimum of $H^+(H_2O)_{21}$.[1,4,5] Subsequent molecular dynamics simulations confirm this picture but indicate that, as a result of the finite temperature of the cluster, isomers other than the global minimum also contribute to the observed spectrum.[10]

For the neutral $(H_2O)_{20}$ cluster, the most stable dodecahedral isomer lies about 10 kcal/mol above the global minimum isomer which has a pentagonal prism (PP) structure.[11,12] This would seem to suggest that the presence of the proton is the key to the high stability of the dodecahedrally derived global minimum isomer of $H^+(H_2O)_{21}$. However, Lee and Beauchamp have observed a magic number at $n = 21$ for [tetrabutylammonium $+ (H_2O)_n]^+$ clusters,[13] and since the charge in this mixed cluster is associated with the amine, this suggests that the water molecules are present as an $(H_2O)_{21}$ cluster with especially high stability. Although $H^+(H_2O)_{21}$ and $(H_2O)_{20}$ have been the subject of numerous theoretical studies, the neutral $(H_2O)_{21}$ cluster has received much less attention. Wales and Hodges have characterized $(H_2O)_{21}$ using the TIP4P water model[14] and reported that the global minimum has a "flat" structure comprised of fused four- and five-membered rings[11] and hereafter referred to as TIP4P-gm(21). More recently, Hartke[15] showed, using the polarizable TTM2-F[16] model potential, that there is a lower energy isomer based on the $(H_2O)_{20}$ water dodecahedron with an interior water molecule engaged in four H-bonds. We refer to this species as DD*(20,1), where the "DD" denotes distorted dodecahedron and the numbers in parentheses indicate that there is one water monomer inside the $(H_2O)_{20}$ dodecahedral cage. The asterisk is to distinguish this isomer from the closely related DD(20,1) isomer considered in the present work and which lies only 0.6 kcal/mol above the DD*(20,1) isomer. These two isomers can be interconverted by six donor−acceptor exchanges of the H-bonding network of the water molecules on the surface of the cluster.

In this paper, we present a detailed theoretical study of the TIP4P-gm(21) and DD(20,1) isomers of $(H_2O)_{21}$, with an emphasis on elucidating the level of theory needed to describe the relative stability of the two isomers. Results are reported for the B3LYP density functional[17−19] and the resolvent-of-the-identity second-order Møller−Plesset perturbation theory (RIMP2)[20,21] electronic structure methods, as well as for the TIP4P[14] effective 2-body model potential and for the Dang−Chang (DC),[22] AMOEBA,[23] and TTM2-F[16] polarizable water models.

We also report the 1-, 2-, 3-, and 4-body contributions,[24] ΔE_1, ΔE_2, ΔE_3, and ΔE_4, respectively, to the net interaction energies. These are defined as

$$\Delta E_1 = \sum_{i=1}^{N} E(i) - nE_w$$

$$\Delta E_2 = \sum_{i=1}^{N-1} \sum_{j=i+1}^{N} [E(i,j) - E(i) - E(j)]$$

† Part of the special issue "Robert J. Silbey Festschrift".

* To whom correspondence should be addressed. E-mail: jordan@pitt.edu.

10.1021/jp056416m CCC: $33.50
Published on Web 03/09/2006

$$\Delta E_3 = \sum_{i=1}^{N-2}\sum_{j=i+1}^{N-1}\sum_{k=j+1}^{N}[E(i,j,k) - E(i,j) - E(i,k) - E(j,k) + E(i) + E(j) + E(k)]$$

$$\Delta E_4 = \sum_{i=1}^{N-3}\sum_{j=i+1}^{N-2}\sum_{k=j+1}^{N-1}\sum_{l=k+1}^{N}[E(i,j,k,l) - E(i,j,k) - E(i,j,l) - E(i,k,l) - E(j,k,l) + E(i,j) + E(i,k) + E(i,l) + E(j,k) + E(j,l) + E(k,l) - E(i) - E(j) - E(k) - E(l)]$$

where $E(i)$, $E(i,j)$, $E(i,j,k)$, and $E(i,j,k,l)$ are, respectively, the energies of the monomer i, dimer (i,j), trimer (i,j,k), and tetramer (i,j,k,l) cut out of the full cluster and E_w is the energy of the monomer at its optimized geometry. ΔE_1, thus, gives the relaxation energy associated with the distortion of the monomers in going from the gas phase to the cluster. For the rigid monomer TIP4P and DC models, ΔE_1 is zero.

There is a twofold motivation for examining the individual n-body contributions. First, the decomposition of the interaction energies into their n-body components provides additional insight into the importance of various terms in the intermolecular potential for determining the relative stability of different isomers. Second, $(H_2O)_{21}$ is an excellent test case for the n-body decomposition method for calculating MP2-level interaction energies.[25] This method exploits the rapid convergence of the n-body expansion of the interaction energy of water cluster,[26,27] approximating the total interaction (binding) energy as $\Delta E \approx \Delta E_1 + \Delta E_2 + \Delta E_3$ or $\Delta E \approx \Delta E_1 + \Delta E_2 + \Delta E_3 + \Delta E_4$.

To date, the largest cluster to which this approach has been applied using MP2-level interaction energies is the hexamer.[25] By applying it to a cluster containing 21 water molecules, we can explore the viability of distance-dependent screening strategies for identifying 3- and 4-body terms that can be neglected, thereby reducing the computational costs. Examination of the n-body contributions also provides new insights into the suitability of density functional methods and of various model potentials for describing the relative stabilities of different isomers of water clusters.

2. Computational Details

The geometries of the two $(H_2O)_{21}$ isomers and of three forms of $(H_2O)_{20}$ included for comparison and described below were optimized using each of the theoretical methods considered. The geometry optimizations with the B3LYP and RIMP2 procedures were performed using the aug-cc-pVDZ basis sets.[28,29] These were followed by single-point calculations using the more flexible aug-cc-pVTZ(-f) basis set, where the $-f$ indicates that the f functions on the O atoms and the d functions on the H atoms that would be present in the full aug-cc-pVTZ basis set have been omitted. The B3LYP and RIMP2 calculations were carried out using Gaussian 03[30] and Turbomole,[31,32] respectively. The calculations with the TIP4P, DC, and AMOEBA force fields were carried out using the Tinker program,[23,33−35] and the calculations with the TTM2-F force field were carried out using the Occident program.[16]

The DC model is a rigid monomer model, using three point charges to represent the electrostatics, a single isotropic polarizable site, and OO Lennard-Jones interactions. This model places positive point charges on each H atom and the balancing negative point charge on the so-called M site, which is located on the rotational axis, displaced 0.215 Å from the O atom toward the H atoms. The isotropic polarizable center is also located at the M site.

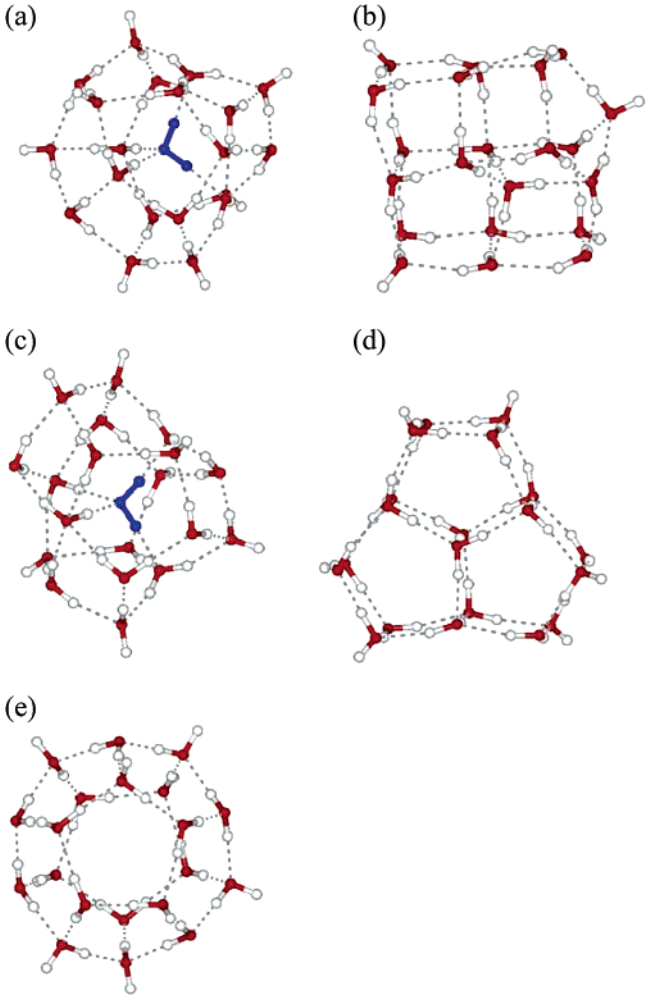

Figure 1. RIMP2/aug-cc-pVDZ optimized geometries of the (a) DD(20,1) and (b) TIP4P-gm(21) isomers of $(H_2O)_{21}$ and of the (c) D(19,1), (d) pentagonal prism [PP(20)], and (e) "perfect" dodecahedron [PD(20)] isomers of $(H_2O)_{20}$.

The TTM2-F and AMOEBA models employ flexible monomers and three atom-centered, mutually interacting, polarizable sites. The TTM2-F model, like the DC model, represents the charge distribution by three point charges (with the positive charges on the H atoms and the negative charge on the M site), whereas the AMOEBA model employs distributed multipoles through quadrupoles on the three atoms. The TTM2-F model uses R^{-12}, R^{-10}, and R^{-6} terms between the O atoms to represent the dispersion interactions and short-range repulsion, while the AMOEBA model employs buffered 7-14 OO, HH, and HO potentials to represent these interactions. Both the AMOEBA and TTM2-F models use a Thole-type damping[36] of the charge−induced dipole interactions and also of the induced dipole−induced dipole interactions. The TTM2-F model damps the charge−charge interactions as well. All three of these polarizable models give values of the dipole and quadrupole moments of the water monomer close to the corresponding experimental values and have been applied with considerable success to water clusters as well as to bulk water.[16,22,23,33]

The two low-energy isomers of $(H_2O)_{21}$ considered in this work are shown in Figure 1. As noted above, these are the global minimum located with the TIP4P model potential and designated TIP4P-gm(21) and an isomer designated DD(20,1) to indicate that it can be viewed as a distorted dodecahedron with an interior water molecule.

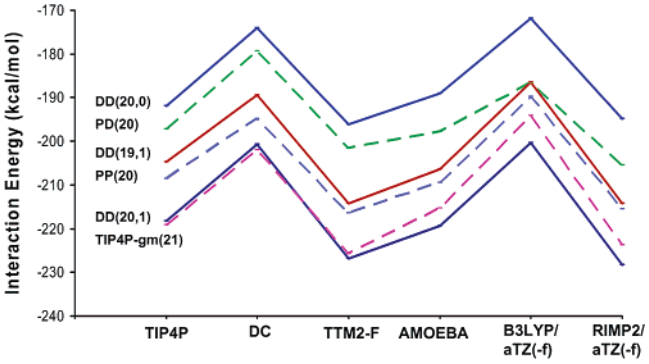

Figure 2. Interaction energies for the DD(20,1) and TIP4P-gm(21) isomers of $(H_2O)_{21}$ and of the various forms of $(H_2O)_{20}$ calculated using the TIP4P, DC, TTM2-F, AMOEBA, B3LYP/aug-cc-pVTZ(-f), and RIMP2/aug-cc-pVTZ(-f) methods.

To aid in analyzing the results for $(H_2O)_{21}$, we also considered the four structures for $(H_2O)_{20}$ shown in Figure 1. These include the "perfect" dodecahedron [PD(20)], the pentagonal prism [PP(20)], the DD(19,1) isomer, which is formed by removing a water from the surface of DD(20,1) and allowing for geometrical relaxation, and a structure designated DD(20,0), formed by removing the interior water molecule from DD(20,1), without allowing relaxation of the geometry.

The *n*-body decomposition was performed by calculating the energies of the various monomers, dimers, trimers, and tetramer subclusters present in the $(H_2O)_{21}$ clusters. The energies from the subcluster calculations were used to evaluate the 2-, 3-, and 4-body interaction energies as a function of a variable *L*, taken to be the sum of the distances from the center of mass of the subcluster to the individual centers of mass of the monomers in the subcluster. *L* thus provides a measure of the "size" of the subcluster. In the electronic structure calculations of the individual *n*-body interaction energies, the full aug-cc-pVTZ basis set was employed for the RIMP2 and B3LYP calculations, with the exception of the B3LYP 4-body results, which were obtained with the aug-cc-pVDZ basis set. In a subset of the electronic structure calculations, the counterpoise correction for basis set superposition error (BSSE)[37] was applied. The discussion will explicitly indicate when the results include the counterpoise correction.

3. Results and Discussion

(i) Energies of the Isomers. Figure 2 reports at various levels of theory the interaction energies calculated for the TIP4P-gm(21) and DD(20,1) isomers of $(H_2O)_{21}$ as well as for the four forms of $(H_2O)_{20}$ described above. From this figure, it is seen that the B3LYP/aug-cc-pVTZ(-f) and RIMP2/aug-cc-pVTZ(-f) calculations place the DD(20,1) isomer energetically below the TIP4P-gm(21) isomer by 6.3 and 4.6 kcal/mol, respectively. (The energy difference between the two isomers was 6.7 kcal/mol at the B3LYP/aug-cc-pVDZ level and 4.2 kcal/mol at the RIMP2/aug-cc-pVDZ level.) The inclusion of corrections for vibrational zero-point energy (estimated at the B3LYP/6-31+G(d) level) further stablizes the DD(20,1) structure over the TIP4P-gm(21) isomer by 1.2 kcal/mol.

At the RIMP2/aug-cc-pVDZ level of theory, the counterpoise correction for BSSE is 43.1 kcal/mol for both the DD(20,1) and TIP4P-gm(21) isomers. The corresponding corrections are 28.1 and 27.5 kcal/mol at the RIMP2/aug-cc-pVTZ(-f) level. Thus, although the counterpoise corrections are large, they are nearly identical for the two isomers, for both basis sets considered. As a result, we conclude that the DD(20,1) isomer of $(H_2O)_{21}$ would be about 4 kcal/mol more stable than the TIP4P-gm(21) isomer in the complete basis set limit (neglecting corrections for vibrational zero-point energy).

The TTM2-F and AMOEBA models favor the DD(20,1) isomer over the TIP4P-gm(21) isomer by 1.1 and 4.0 kcal/mol, respectively. On the other hand, the TIP4P and DC models both predict the TIP4P-gm(21) isomer to be slightly (0.8−1.2 kcal/mol) more stable than the DD(20,1) isomer. Since a major difference between the DC and TTM2-F models is the switch from a single polarizable site in the former to distributed polarizable sites in the latter, it is tempting to conclude that in a model potential approach use of distributed polarizable sites is necessary in order to properly describe the energy difference between the TIP4P-gm(21) and DD(20,1) isomers of $(H_2O)_{21}$. However, we will see later, other factors appear to be responsible for the incorrect ordering obtained with the DC model.

For the $(H_2O)_{20}$ cluster, the PP(20) isomer is lowest in energy at all levels of theory considered. The energy gap between the PP(20) and DD(19,1) isomer of $(H_2O)_{20}$ is only 1.3 kcal/mol at the RIMP2/aug-cc-pVTZ(-f) level. The DD(20,0) species is calculated to be less stable by 5−15 kcal/mol, depending on the theoretical method employed, than the PD(20) isomer. This difference represents the energetic cost of distorting the $(H_2O)_{20}$ dodecahedron from its ideal structure to the structure it has in the DD(20,1) isomer. The DD(20,1) species is calculated to be 26−35 kcal/mol more stable than the DD(20,0) species. Thus, although there is a considerable energy cost for distorting the ideal dodecahedron to DD(20), in particular, for rotating two of the free OH groups inward, this is more than compensated for by the four new H-bonds between the internal water molecule and the $(H_2O)_{20}$ cage. The energy differences obtained using the TTM2-F and AMOEBA models are in fairly good agreement with each other and with the RIMP2/aug-cc-pVTZ(-f) values. However, there are some significant differences between the relative energies from the B3LYP and RIMP2 calculations. For example, the B3LYP/aug-cc-pVTZ(-f) calculations predict DD(19,1) to be 0.1 kcal/mol less stable than PD(20), whereas the RIMP2/aug-cc-pVTZ(-f) calculations predict DD(19,1) to be more stable by 8.8 kcal/mol. This may be a consequence of the inadequency of the density functional methods for describing long-range dispersion interactions.[37]

(ii) *n*-Body Interaction Energies. The net 2-, 3- and 4-body interaction energies calculated for the TIP4P-gm(21) and DD(20,1) isomers of $(H_2O)_{21}$ cluster are summarized in Table 1. The distance dependence of these quantities is explored in Figures 3−5 which report the cumulative *n*-body interaction energies as a function of *L*. The B3LYP and RIMP2 results reported in Table 1 and in Figures 3−5 were obtained with the aug-cc-pVTZ basis set and without the counterpoise correction for BSSE. The *n*-body contributions were also calculated using the aug-cc-pVTZ(-f) basis set but were found to be very close to those obtained with the full aug-cc-pVTZ basis set, so only the latter results are reported.

From Table 1, it is seen that the TTM2-F force field gives net 2-body interaction energies close to the corresponding RIMP2/aug-cc-pVTZ values. In contrast, the DC and AMOEBA force field models and the B3LYP/aug-cc-pVTZ DFT calculations considerably underestimate (by 16−35 kcal/mol) the magnitude of the net 2-body interaction energies. A rather different picture emerges for the 3- and 4-body energies. Whereas the AMOEBA force field gives net 3-body energies fairly close to the RIMP2/aug-cc-pVTZ results, the DC and TTM2-F methods give net 3-body energies 10.6−14.4 kcal/mol smaller and the B3LYP method gives the 3-body energies

TABLE 1: *n*-body Interaction Energies (kcal/mol) for the TIP4P-gm(21) and DD(20,1) isomers of $(H_2O)_{21}$[a]

	TIP4P-gm(21)				DD(20, 1)			
theoretical method	1-body	2-body	3-body	4-body	1-body	2-body	3-body	4-body
DC	0.00	−164.08	−35.94	−1.98	0.00	−161.05	−36.66	−3.02
TTM2-F	4.12	−191.84	−36.66	−1.79	4.39	−190.88	−37.38	−3.23
AMOEBA	5.90	−173.25	−46.34	−2.44	6.26	−172.74	−48.63	−4.70
B3LYP/aug-cc-pVDZ	8.06	−155.09	−55.70	−2.45	10.49	−155.54	−60.97	−6.32
B3LYP/aug-cc-pVTZ	10.15	−147.60	−56.59		12.65	−148.05	−62.17	
RIMP2/aug-cc-pVTZ	10.87	−189.68	−47.21	−9.10	12.95	−189.16	−51.07	−11.26

[a] The DC, TTM2-F, AMOEBA, and B3LYP/aug-cc-pVDZ results are reported at geometries optimized using the respective methods. The B3LYP/aug-cc-pVTZ and RIMP2/aug-cc-pVTZ results were obtained using B3LYP/aug-cc-pVDZ and RIMP2/aug-cc-pVDZ optimized geometries, respectively.

8.5−9.9 kcal/mol larger in magnitude than the corresponding RIMP2/aug-cc-pVTZ results. At the MP2/aug-cc-pVTZ level, the 3-body energies for the TIP4P-gm(21) and DD(20,1) isomers are −47.2 and −51.1 kcal/mol, respectively. On a per monomer base, this translates to −2.2 and −2.4 kcal/mol, respectively. Thus, 3-body interactions play a major role in the stabilization of DD(20,1) relative to TIP4P-gm(21). Both the DC and TTM2-F models give a 3-body energy of the DD(20,1) isomer only 0.7 kcal/mol greater in magnitude than that for the TIP4P-gm(21) isomer, a much smaller difference than that found with the AMOEBA model and with either electronic structure method. Similar behavior is found in the 4-body energies, discussed below. Since the 3- and 4-body interaction energies are dominated by polarization effects, these results indicate that both the DC and TTM2-F models are "underpolarized". Moreover, the nearly identical 3- and 4-body contributions obtained with the DC and TTM2-F models indicate that the incorrect energy ordering with DC model is not solely the consequence of its use of a single polarizable site. Indeed, from Table 1 it is seen that the 2-body interactions play a major role in favoring TIP4P-gm(21) over DD(20,1) with the DC model.

All three polarizable model potentials and the B3LYP method give net 4-body interaction energies appreciably smaller in magnitude than those from the RIMP2 calculations. The net 4-body energies obtained with the model potentials range from −1.8 to −4.7 kcal/mol, and the B3LYP 4-body energies are somewhat larger in magnitude. The DC and TTM2-F methods give similar 4-body energies, somewhat smaller in magnitude than the AMOEBA results.

Figure 3 reports the variation with L of the 2-body energies calculated with the various theoretical methods. For the TIP4P-gm(21) isomer, the 2-body energies are well converged at $L =$ 5 Å, but for the DD(20,1) isomer, it is necessary to sum the 2-body energies out to $L = 7$ Å to get a well-converged 2-body energy. It is also seen from this figure that the discrepancies of the DC, AMOEBA, and B3LYP 2-body energies from the corresponding RIMP2 results arise primarily from the $L \leq 5$ Å contributions.

Figure 4 reports the cumulative 3-body energies as a function of L. From this figure, it is seen that to a large extent the differences between the net 3-body energies calculated using different theoretical methods are due to the short-range ($L < 6$ Å) contributions. It is also seen that it is necessary to sum contributions up to $L = 10$ Å to achieve convergence of the 3-body energies.

Figure 5 displays the variation with L of the cumulative 4-body interaction energies calculated using the various theoretical methods. Whereas the AMOEBA and TTM2-F 4-body energies are fairly well converged when contributions out to $L = 13$ Å are summed, the 4-body energies calculated using the RIMP2 procedure continue to grow in magnitude as L is increased out to about 15 Å. The B3LYP 4-body energy also

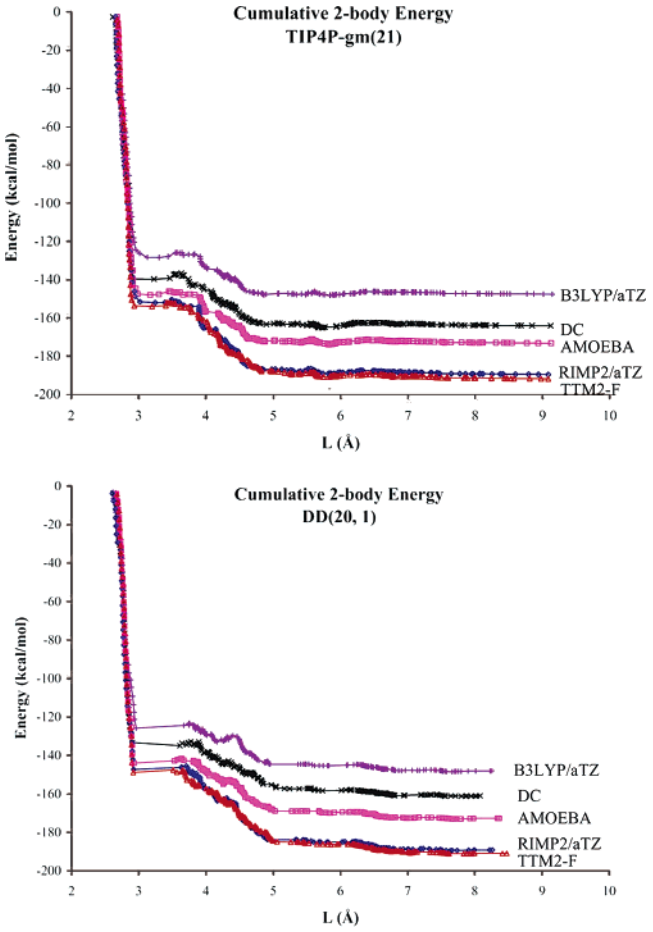

Figure 3. Cumulative 2-body interaction energies vs distance L for the TIP4P-gm(21) and DD(20,1) isomers of $(H_2O)_{21}$.

grows more rapidly at large L than do the model potential results but to a far lesser extent than does the RIMP2 4-body energy. The long-range "divergence" of the RIMP2 4-body energy with increasing L is even more rapid when using the aug-cc-pVDZ basis set (results not included in the figure), indicating that BSSE[37] is partially responsible for the unexpected behavior of the RIMP2 4-body energy. (This is substantiated by examining the Hartree−Fock results which have not been reported in the figure.)

To gain additional insight into the origin of the surprisingly large 4-body interactions in the RIMP2 calculations, we examine in detail six tetramers cut out of the DD(20,1) cluster. The structures of these tetramers, which have L values ranging from 9.2 to 16 Å, are shown in Figure 6, and the associated 4-body interaction energies are given in Table 2. For three of the tetramers, **A**, **B**, and **E**, the RIMP2-level 4-body energy displays a strong basis set dependence. For example, for tetramer **A**, the RIMP2-level 4-body interaction energy is calculated to be

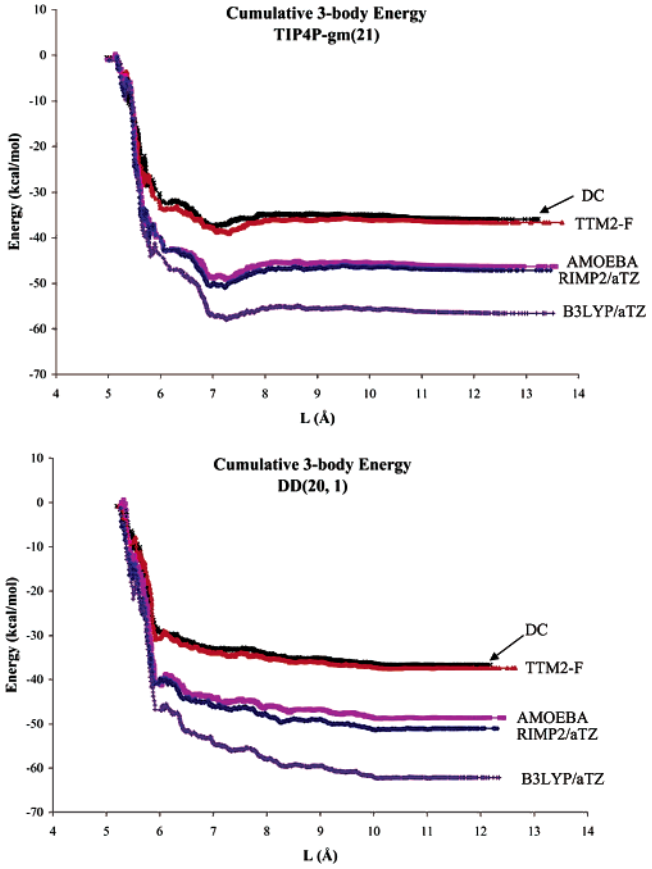

Figure 4. Cumulative 3-body interaction energies vs distance for the TIP4P-gm(21) and DD(20,1) isomers of $(H_2O)_{21}$.

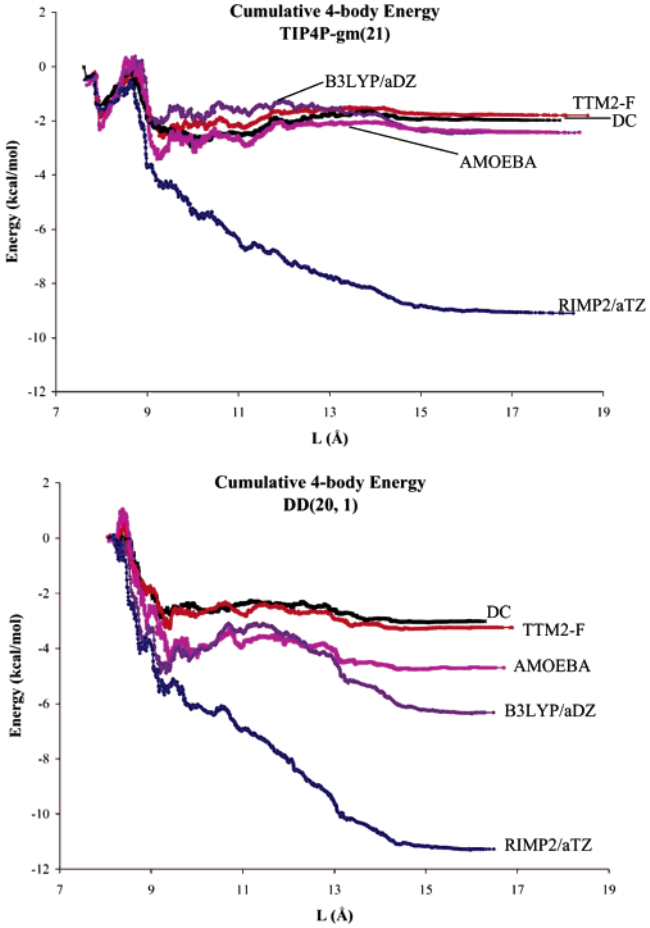

Figure 5. Cumulative 4-body interaction energies vs distance for the TIP4P-gm(21) and DD(20,1) isomers of $(H_2O)_{21}$.

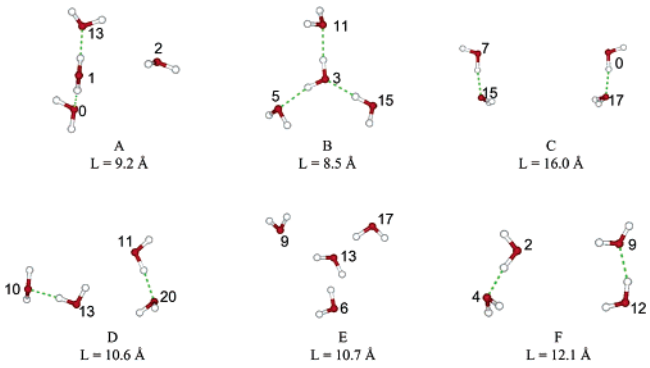

Figure 6. Tetramers selected from the RIMP2/aug-cc-pVDZ optimized structure of the DD(20,1) isomer of $(H_2O)_{21}$.

−0.011, 0.007, and 0.009 kcal/mol with the aug-cc-pVDZ, aug-ccpVTZ, and aug-cc-pVQZ basis sets,[28,29] respectively. The counterpoise-corrected value is 0.014 kcal/mol with both the aug-cc-pVDZ and aug-cc-pVTZ basis sets, leading us to conclude that the complete-basis-set-limit MP2-level interaction energy is about 0.014 kcal/mol for this tetramer. For tetramers **C**, **D**, and **F**, the RIMP2-level 4-body interaction energies are relatively insensitive to the basis set. The main difference between these two groups of tetramers is that **A**, **B**, and **E** all contain a water trimer with short nearest-neighbor OO distances, whereas **C**, **D**, and **F** can be viewed as two interacting dimers. It should be noted that although the errors due to BSSE to the individual 4-body contributions as calculated with the RIMP2 procedure are quite small (0.014 kcal/mol or smaller), there are 5985 such terms so that the contribution of BSSE to the net 4-body RIMP2/aug-cc-pVTZ interaction energy is sizable.

For four of the sampled tetramers, **A**, **B**, **D**, and **F**, the RIMP2 values of the 4-body interaction energies are more attractive (or less repulsive), even after application of the counterpoise correction, than are the results from either of the AMOEBA or TTM2-F force fields. For example, for isomer **D**, the counterpoise-corrected RIMP2 value of the 4-body interaction energy is −0.065 kcal/mol, whereas the corresponding AMOEBA and TTM2-F values are −0.016 and −0.010 kcal/mol, respectively.

It is clear from the results discussed above that the discrepancies between the 4-body interaction energies calculated with the RIMP2 procedure and with the model potentials have two causes: (1) the BSSE in the RIMP2 energies due to the truncation of the basis set and (2) inadequacy of the polarizable model potentials to capture all of the "physics" of the interactions. Of these, the second factor is the more important one. The greater attraction of the RIMP2 4-body energies compared to the corresponding Hartree−Fock, B3LYP, TTM2-F, and AMOEBA results suggests interactions that couple dispersion and induction may be important. Such interactions would contribute to the MP2 4-body energies but not to those calculated using the model potentials or using the Hartree−Fock or B3LYP methods.

In light of the discrepancies between the model potential and RIMP2 results for the 4-body energies, it is instructive to take a closer look at the 3-body contributions. To this end, we summarize in Table 3 the 3-body energies for nine trimers cut out of the DD(20,1) isomer. It is seen from these results that the RIMP2 3-body energies calculated with the aug-cc-pVTZ and aug-cc-pVQZ basis sets are in excellent agreement. (Indeed, even the results obtained with the aug-cc-pVDZ basis set are in good overall agreement with those obtained using the aug-

TABLE 2: 4-body Interaction Energies (kcal/mol) of Selected Tetramers from DD(20,1)[a,b]

cluster[c]	*L* (Å)	RIMP2/aDZ	RIMP2/aTZ(-f)	RIMP2/aTZ	RIMP2/aQZ	AMOEBA	TTM2-F
A	9.184	−0.011	0.004	0.007	0.009	0.024	0.021
		(0.013)	(0.014)	(0.014)			
B	8.490	−0.033	−0.008	−0.006	−0.002	0.044	0.029
		(0.008)	(0.008)	(0.008)			
C	15.990	0.027	0.027	0.029	0.029	0.026	0.015
		(0.029)	(0.029)	(0.029)			
D	10.555	−0.061	−0.067	−0.066	−0.065	−0.016	−0.010
		(−0.066)	(−0.066)	(−0.065)			
E	10.671	−0.018	−0.011	−0.010	−0.006	−0.001	−0.002
		(−0.002)	(−0.002)	(−0.001)			
F	12.109	−0.063	−0.062	−0.063	−0.063	−0.051	−0.033
		(−0.062)	(−0.063)	(−0.062)			

[a] aDZ, aTZ, and aQZ denote the aug-cc-pVDZ, aug-cc-pVTZ, and aug-cc-pVQZ basis sets, respectively. [b] Results in parentheses include the counterpoise correction for basis set superposition error. [c] The selected tetramers are shown in Figure 6.

TABLE 3: 3-body Interaction Energies (kcal/mol) of Selected Trimers from DD(20,1)[a]

cluster[b]	*L* (Å)	RIMP2/aDZ	RIMP2/aTZ	RIMP2/aQZ	AMOEBA	TTM2-F
1_2_13 (A)	6.21	−0.23	−0.27	−0.27	−0.23	−0.20
0_1_13 (A)	5.59	0.95	0.91	0.92	0.98	0.67
3_11_15 (B)	5.86	−0.99	−1.01	−1.01	−1.05	−0.75
3_5_11 (B)	5.84	1.04	1.03	1.05	1.08	0.68
0_7_15 (C)	11.09	0.04	0.04	0.04	0.04	0.03
11_13_20 (D)	6.22	−0.43	−0.44	−0.44	−0.37	−0.32
10_11_13 (D)	7.19	0.04	0.04	0.04	0.10	0.05
6_9_13 (E)	7.44	0.02	0.01	0.02	0.00	−0.01
2_4_9 (F)	7.97	−0.18	−0.18	−0.18	−0.12	−0.10

[a] aDZ, aTZ, and aQZ denote the aug-cc-pVDZ, aug-cc-pVTZ, and aug-cc-pVQZ basis sets, respectively. [b] The selected trimers are contained within the tetramers shown in Figure 6.

cc-pVQZ basis set.) This shows that BSSE is relatively unimportant for the 3-body RIMP2/aug-cc-pVTZ energies. In other words, although in an absolute sense corrections for BSSE tend to be more important for the 3-body interaction energies than for the 4-body interaction energies, on a percentage basis they are more important for the 4-body interaction energies. Similarly, although coupled induction−dispersion interactions are probably more important in an absolute sense for the 3-body than for the 4-body interaction energy, they do not cause a large *L* "divergence" of the former because of the dominance of the 3-body polarization interactions.

Overall, there is fairly good agreement between the AMOEBA and RIMP2/aug-cc-pVQZ values of the 3-body energies, although the AMOEBA force field considerably underestimates (by up to 33%) the magnitude of the 3-body energies for trimers with a D−AD−A arrangement, where D and A denote donor and acceptor monomers, respectively. In general, the deviations from the RIMP2 values are even greater with the TTM2-F model than with the AMOEBA model. There are several possible factors that could contribute to the deviations of the 3-body energies calculated using the model potentials from those calculated using the RIMP2 method. These include the previously mentioned neglect of coupling between induction and dispersion in the model potentials, as well as errors introduced by limiting polarization to dipole terms and by the use of point charges (TTM2-F) or a truncated distributed multipole expansion (AMOEBA) in representing the charge distributions of the monomers.

4. Conclusions

Two low-energy forms of the $(H_2O)_{21}$ cluster have been examined theoretically using both model potentials and electronic structure methods. Both the RIMP2 and the B3LYP density functional methods predict that the DD(20,1) isomer, derived from a water dodecahedron, is more stable than the TIP4P-gm(21) isomer. The TTM2-F and AMOEBA force fields, both of which employ atom-centered distributed polarizabilities, also predict the DD(20,1) isomer to be more stable than the TIP4P-gm(21) isomer, with the energy separation from the AMOEBA calculations agreeing more closely with the RIMP2 result. On the other hand, the 2-body TIP4P and DC models predict the TIP4P-gm(21) isomer to be slightly more stable than DD(20,1). The latter two model potentials considerably underestimate the magnitude of the 3- and 4-body interaction energies (compared with the RIMP2 results), whereas the AMOEBA model gives results closer to those of the RIMP2 calculations, particularly for the 3-body interaction energies. It is also found that the B3LYP procedure, while underestimating the 2-body interaction energies, significantly overestimates the 3-body interaction energies.

The RIMP2 procedure gives much larger (in magnitude) 4-body interaction energies than those obtained with any of the other methods. It is demonstrated that this is partly the result of basis set superposition error. However, more interestingly, part of the discrepancy is due to contributions to the 4-body energies that are present in the MP2 calculations but which are absent in the model potentials and B3LYP approaches. We speculate that this is a consequence of mixed dispersion−induction interactions that would be present in the MP2 calculations but not in the other methods. We plan to examine this issue in more detail in a future study. We are unaware of any studies that have examined the importance of dispersion−induction coupling in water clusters. The SAPT method[38] would be a natural framework in which to analyze such interactions.

Although the present work reveals that it is difficult to achieve well-converged 4-body interaction energies, it should be kept in mind that the 4-body contributions to the net interaction energies are relatively small, and their complete neglect would introduce an error of only ∼2 kcal/mol in the relative energy of the TTM-gm(21) and DD(20,1) isomers of $(H_2O)_{21}$. More-

over, even though the model potentials considerably underestimate the 4-body interaction energies, in magnitude, they fare much better (especially the AMOEBA model) at describing the relative 4-body interaction energies.

Finally, we examined the convergence of the various *n*-body contributions as a function of a distance parameter *L*. This analysis reveals that the large *L* contributions to the 3- and 4-body energies are relatively unimportant. However, if we choose *L* values such that the resulting 3- and 4-body energies are within 1 kcal/mol of convergence, we find that it is necessary to evaluate about three-quarters of all possible contributions. Hence, for clusters the size of $(H_2O)_{21}$, this screening approach does not lead to a large reduction in computational time required for calculating RIMP2-level interaction energies via the *n*-body decomposition procedure.

Acknowledgment. This research was carried out with the support of the National Science Foundation (Grant No. CHE-0518253). The calculations were carried out on computers in the University of Pittsburgh's Center for Molecular and Materials Simulations.

References and Notes

(1) Shin, J. W.; Hammer, N. I.; Diken, E. G.; Johnson, M. A.; Walters, R. S.; Jaeger, T. D.; Duncan, M. A.; Christie, R. A.; Jordan, K. D. *Science* **2004**, *304*, 1137.

(2) Miyazaki, M.; Fujii, A.; Ebata, T.; Mikami, N. *Science* **2004**, *304*, 1134.

(3) Wu, C.-C.; Lin, C.-K.; Chang, H.-C.; Jiang, J.-C.; Kuo, J.-L.; Klein, M. L. *J. Chem. Phys.* **2005**, *122*, 074315.

(4) Kuo, J.-L.; Klein, M. L. *J. Chem. Phys.* **2005**, *122*, 024516.

(5) James, T.; Wales, D. J. *J. Chem. Phys.* **2005**, *122*, 134306.

(6) Searcy, J. Q.; Fenn, J. B. *J. Chem. Phys.* **1974**, *61*, 5282.

(7) Wei, S.; Shi, Z.; Castleman, A. W., Jr. *J. Chem. Phys.* **1991**, *94*, 3268.

(8) Lee, S. W.; Cox, H.; Goddard, W. A.; Beauchamp, J. L. *J. Am. Chem. Soc.* **2000**, *122*, 9201.

(9) Niedner-Schatteburg, G.; Bondybey, V. E. *Chem. Rev.* **2000**, *100*, 4059.

(10) Iyengar, S. S.; Petersen, M. K.; Day, T. J. F.; Burnham, C. J.; Teige, V. E.; Voth, G. A. *J. Chem. Phys.* **2005**, *123*, 084309.

(11) Wales, D. J.; Hodges, M. P. *Chem. Phys. Lett.* **1998**, *286*, 65.

(12) Fanourgakis, G. S.; Apra, E.; Xantheas, S. S. *J. Chem. Phys.* **2004**, *121*, 2655.

(13) Lee, S. W.; Freivogel, P.; Schindler, T.; Beauchamp, J. L. *J. Am. Chem. Soc.* **1998**, *120*, 11758.

(14) Jorgensen, W. L.; Chandrasekhar, J.; Madura, J. D.; Impey, R. W.; Klein, M. L. *J. Chem. Phys.* **1983**, *79*, 926.

(15) Hartke, B. *Phys. Chem. Chem. Phys.* **2003**, *5*, 275.

(16) Burnham, C. J.; Xantheas, S. S. *J. Chem. Phys.* **2002**, *116*, 5115.

(17) Becke, A. D. *J. Chem. Phys.* **1993**, *98*, 5648.

(18) Lee, C.; Yang, W.; Parr, R. G. *Phys. Rev. B* **1988**, *37*, 785−789.

(19) Gill, P. M. W.; Johnson, B. G.; Pople, J. A.; Frisch, M. J. *Chem. Phys. Lett.* **1992**, *197*, 499.

(20) Feyereisen, M.; Fitzgerald, G.; Komornicki, A. *Chem. Phys. Lett.* **1993**, *208*, 359.

(21) Bernholdt, D. E.; Harrison, R. J. *Chem. Phys. Lett.* **1996**, *250*, 477.

(22) Dang, L. X.; Chang, T.-M. *J. Chem. Phys.* **1997**, *106*, 8149.

(23) Ren, P. Y.; Ponder, J. W. *J. Phys. Chem. B* **2003**, *107*, 5933.

(24) Xantheas, S. S. *J. Chem. Phys.* **1994**, *100*, 7523.

(25) Christie, R. A.; Jordan, K. D. *Intermolecular Forces*; Wales, D., Ed.; Springer: New York, 2005.

(26) Christie, R. A.; Jordan, K. D. *J. Phys. Chem. A* **2001**, *105*, 7551.

(27) Pedulla, J. M.; Kim, K.; Jordan, K. D. *Chem. Phys. Lett.* **1998**, *291*, 78.

(28) Kendall, R. A.; Dunning, T. H.; Harrison, R. J. *J. Chem. Phys.* **1992**, *96*, 6796.

(29) Dunning, T. H. *J. Chem. Phys.* **1989**, *90*, 1007.

(30) Frisch, M. J.; Trucks, G. W.; Schlegel, H. B.; Scuseria, G. E.; Robb, M. A.; Cheeseman, J. R.; Montgomery, J. A., Jr.; Vreven, T.; Kudin, K. N.; Burant, J. C.; Millam, J. M.; Iyengar, S. S.; Tomasi, J.; Barone, V.; Mennucci, B.; Cossi, M.; Scalmani, G.; Rega, N.; Petersson, G. A.; Nakatsuji, H.; Hada, M.; Ehara, M.; Toyota, K.; Fukuda, R.; Hasegawa, J.; Ishida, M.; Nakajima, T.; Honda, Y.; Kitao, O.; Nakai, H.; Klene, M.; Li, X.; Knox, J. E.; Hratchian, H. P.; Cross, J. B.; Bakken, V.; Adamo, C.; Jaramillo, J.; Gomperts, R.; Stratmann, R. E.; Yazyev, O.; Austin, A. J.; Cammi, R.; Pomelli, C.; Ochterski, J. W.; Ayala, P. Y.; Morokuma, K.; Voth, G. A.; Salvador, P.; Dannenberg, J. J.; Zakrzewski, V. G.; Dapprich, S.; Daniels, A. D.; Strain, M. C.; Farkas, O.; Malick, D. K.; Rabuck, A. D.; Raghavachari, K.; Foresman, J. B.; Ortiz, J. V.; Cui, Q.; Baboul, A. G.; Clifford, S.; Cioslowski, J.; Stefanov, B. B.; Liu, G.; Liashenko, A.; Piskorz, P.; Komaromi, I.; Martin, R. L.; Fox, D. J.; Keith, T.; Al-Laham, M. A.; Peng, C. Y.; Nanayakkara, A.; Challacombe, M.; Gill, P. M. W.; Johnson, B.; Chen, W.; Wong, M. W.; Gonzalez, C.; Pople, J. A. *Gaussian 03*, revision C.02; Gaussian, Inc.: Wallingford, CT, 2004.

(31) Treutler, O.; Ahlrichs, R. *J. Chem. Phys.* **1995**, *102*, 346.

(32) Von Arnim, M.; Ahlrichs, R. *J. Comput. Chem.* **1998**, *19*, 1746.

(33) Ren, P. Y.; Ponder, J. W. *J. Comput. Chem.* **2002**, *23*, 1497.

(34) Pappu, R. V.; Hart, R. K.; Ponder, J. W. *J. Phys. Chem. B* **1998**, *102*, 9725.

(35) Hodsdon, M. E.; Ponder, J. W.; Cistola, D. P. *J. Mol. Biol.* **1996**, *264*, 585.

(36) Thole, B. T. *Chem. Phys.* **1981**, *59*, 341.

(37) Boys, S. F.; Bernardi, F. *Mol. Phys.* **1970**, *19*, 553.

(38) Mas, E. M.; Szalewicz, K.; Bukowski, R.; Jeziorski, B. *J. Chem. Phys.* **1997**, *107*, 4207.